






Chapter 3

High-precision strong lensing models of galaxy clusters in the JWST era

P. Bergamini^{1,2} , C. Grillo^{1,5}, P. Rosati^{2,3,9}, A. Acebron^{1,5},
E. Vanzella² , A. Mercurio^{4,10}, M. Meneghetti², G. Angora^{3,4} ,
G. Granata^{1,5}, U. Mestric^{1,2}, G. B. Caminha^{6,7} and T. Treu¹¹

¹Dipartimento di Fisica, Università di Milano, via Celoria 16, I-20133 Milano, Italy.
email: pietro.bergamini@unimi.it

²INAF – OAS, Osservatorio di Astrofisica e Scienza dello Spazio di Bologna, via Gobetti 93/3,
I-40129 Bologna, Italy

³Dipartimento di Fisica e Scienze della Terra, Università di Ferrara, Via Saragat 1, I-44122
Ferrara, Italy

⁴INAF – Osservatorio Astronomico di Capodimonte, Salita Moiariello 16, I-80131 Napoli, Italy

⁵INAF – IASF Milano, via A. Corti 12, I-20133 Milano, Italy

⁶Technische Universität München, Physik-Department, James-Franck Str. 1, D-85741
Garching, Germany

⁷Max-Planck-Institut für Astrophysik, Karl-Schwarzschild-Str. 1, D-85748 Garching, Germany

⁸INAF – Osservatorio Astronomico di Trieste, via G. B. Tiepolo 11, I-34131 Trieste, Italy

⁹INFN, Sezione di Ferrara, Via Saragat 1, I-44122 Ferrara, Italy

¹⁰Dipartimento di Fisica, Università di Salerno, Via Giovanni Paolo II, 132, I-84084, Fisciano
(SA), Italy

¹¹Department of Physics and Astronomy, University of California, Los Angeles, 430 Portola
Plaza, Los Angeles, CA 90095, USA

Abstract. We present high-precision strong lensing models for the galaxy clusters MACS J0416.1–0403 at $z = 0.396$ and Abell 2744 at $z = 0.307$. The models are constrained by two of the largest data-sets of secure multiple images ever used in lensing. These are identified from the photometric images observed by the *Hubble* space telescope and *JWST* in combination with spectroscopic data obtained by the Multi-Unit Spectroscopic Explorer at the Very Large Telescope. The same spectro-photometric data are used to create pure and complete samples of cluster member galaxies. Our models allow an extremely precise estimation of the cluster total mass distribution and produce accurate magnification maps that are fundamental to study the physical properties (mass, size, luminosity, etc.) of the lensed high-redshift galaxies.

Keywords. Galaxy Cluster, Strong Gravitational Lensing, Dark Matter

1. Introduction

The currently accepted cosmological model (a.k.a. Λ CDM) assumes that dark energy (DE) and dark matter (DM) are the two dominant components of the Universe, accounting for more than 95% of its total mass-energy budget, while baryonic matter contributes just for $\sim 5\%$. While DE is responsible for the measured accelerated expansion of the Universe, DM is expected to be formed by non-relativistic (cold) and weakly interacting particles whose nature is still unknown. Despite numerous particle physics experiments

were designed to detect the DM particles directly, the only observation evidence of the DM existence remains its gravitational interaction with baryonic matter in astronomical systems.

In this context, the galaxy clusters, which are the largest gravitationally bound structures in the Universe and with the $\sim 85\%$ of their total mass made of DM, represent unique nature laboratories to study the DM particles. In particular, a detailed analysis of the total, baryonic, and DM mass density distributions in the inner region of galaxy clusters can provide stringent constraints on the DM physical properties. In fact, both the slope of the radial profile of the DM in the central region of galaxy clusters and the spatial segregation of the DM subhalos with respect to the baryonic matter are strongly affected by the interaction cross-section of the DM particles. Over the last decade, strong gravitational lensing (SL) has become the most accurate technique to determine the projected total mass distribution of the core region of galaxy clusters. The reasons for its success have to be mainly ascribed to the high-quality spectro-photometric data obtained by the *Hubble* Space Telescope (HST), and by the VIMOS (Visible MultiObject Spectrograph, [Le Fèvre et al. 2003](#)) and MUSE (Multi-Unit Spectroscopic Explorer, [Bacon et al. 2012](#)) spectrographs mounted on the Very Large Telescope (VLT). These data are used to identify large samples of spectroscopically confirmed multiple images (e.g., [Grillo et al. 2016](#); [Karman et al. 2017](#); [Lagattuta et al. 2017](#); [Richard et al. 2021](#); [Bergamini et al. 2021, 2023](#); [Caminha et al. 2016, 2019](#)) and pure and complete catalogs of cluster member galaxies (e.g., [Bergamini et al. 2019](#); [Angora et al. 2020](#)). With the advent of the JWST, a further step forward was possible in the SL modeling of galaxy clusters thanks to the photometric and spectroscopic data of unprecedented quality.

Other than to study the mass distribution of galaxy clusters, the SL can be used to exploit the clusters as cosmic telescopes to study a population of background lensed sources that are the progenitor of the present-day galaxies and globular clusters, and that may have played a fundamental role in the re-ionization of the Universe (e.g., [Vanzella et al. 2017, 2020, 2022, 2023](#); [Meštrić et al. 2022](#); [Roberts-Borsani et al. 2023](#)). In particular, the magnification maps obtained by the SL models are fundamental to derive the intrinsic physical properties of these faint, highly magnified, and high- z sources.

In this contribution, we will present state-of-the-art strong lensing models for the two massive galaxy clusters MACS J0416.1–0403 (hereafter M0416) at $z = 0.396$ and Abell 2744 (hereafter A2744) at $z = 0.307$. Throughout this work, we assume a flat Λ CDM cosmology with $\Omega_m = 0.3$ and $H_0 = 70 \text{ km s}^{-1} \text{ Mpc}^{-1}$.

2. Observational data

The galaxy cluster M0416 was one of the selected targets of the Cluster Lensing And Supernova survey with Hubble (CLASH, [Postman et al. 2012](#)) and Hubble Frontier Fields (HFF, [Lotz et al. 2017](#)) program that provided multi-band HST observations of the cluster. Several spectroscopic campaigns were also carried out on the cluster to complement the photometric data. In particular, the CLASH-VLT (P.I.: Rosati) program provided VLT/VIMOS observations that allowed the measurement of the redshift of thousands of sources over a 20 arcmin^2 field-of-view. The following MUSE pointings were also obtained on the cluster: a MUSE pointing of 2h centered on the northeast (NE) region of the cluster (GTO 094.A-0115B, P.I.: Richard); a MUSE pointing of 11h centered on the southwest (SW) region of the cluster (094.A0525(A), P.I.: Bauer); an ultra-deep MUSE pointing centered on the northeast region of the cluster that, when stacked with previous observations, allows to reach a total exposure time of 17.1h in the NE region (0100.A-0763(A), P.I.: Vanzella, [Vanzella et al. 2021](#)).

Similarly, the HFF program provided deep HST photometric data on the core region of the galaxy cluster A2744, while shallower HST observations on the external regions were obtained during the Beyond Ultra-deep Frontier Fields And Legacy Observations (BUFFALO, Steinhardt et al. 2020) campaign. More recently the cluster was selected as one of the primary targets of the JWST. In particular, NIRC*am* images were taken within the GLASS-JWST program ERS-1324 (P.I.: Treu, Treu et al. 2022), the Ultradeep NIRS*pec* and NIRC*am* Observations before the Epoch of Reionization Cycle 1 Treasury program (UNCOVER, GO-2561, co-P.I.s: Labbè and Bezanson, Bezanson et al. 2022), and the DDT program 2756 (P.I.: Chen). These data were complemented by a total of 10 MUSE pointings of 1 arcmin² each. Five of the pointings are centered in the core region of the cluster and have an exposure time between 2h and 5h (Richard et al. 2021; Mahler et al. 2018), while the other five (co-P.I.s: Mason, Vanzella) have an exposure of 1h each and mostly cover the same area of the GLASS-JWST ERS NIRC*am* observations.

3. Lens modeling technique

To develop the strong lensing models we exploit the publicly available parametric software *LensTool* (Kneib et al. 1996; Jullo et al. 2007; Jullo & Kneib 2009). In parametric software, the total mass distribution of the cluster has to be decomposed into a sum of different parametric components:

$$\phi_{tot} = \sum_{i=1}^{N_h} \phi_i^{halo} + \sum_{j=1}^{N_{gas}} \phi_j^{gas} + \sum_{k=1}^{N_g} \phi_k^{gal} + \phi_{foreg}. \tag{1}$$

The first term of the sum is used to parameterize the large cluster-scale halos of the galaxy cluster that are primarily made of DM. The second term describes the hot gas (baryonic) mass contained in the cluster. The third term accounts for the contribution of the cluster galaxies to the cluster total mass. These are usually described with truncated Singular Isothermal Sphere (tSIS) profiles whose free parameters, i.e., their central velocity dispersion (σ_i) and truncation radius ($r_{cut,i}$), are scaled with the galaxy luminosity (L_i) according to the following two scaling relations:

$$\sigma_i = \sigma^{ref} \left(\frac{L_i}{L_{ref}} \right)^\alpha, \quad r_{cut,i} = r_{cut}^{ref} \left(\frac{L_i}{L_{ref}} \right)^{\beta_{cut}}, \tag{2}$$

where the two normalizations σ^{ref} and r_{cut}^{ref} , and the two slopes α and β_{cut} are free parameters of the lens model. Finally, the fourth term in Eq. 1 is necessary to consider the non-negligible impact that foreground galaxies and/or massive structures residing in the outer region of the cluster have on the lensing observables.

The lens model optimization is performed using a Bayesian approach by looking for the combination of model free parameters, ξ , that minimize the following χ^2 function:

$$\chi^2(\xi) := \sum_{j=1}^{N_{fam}} \sum_{i=1}^{N_{im}^j} \left(\frac{\| \mathbf{x}_{i,j}^{pred}(\xi) - \mathbf{x}_{i,j}^{obs} \|}{\Delta x_{i,j}} \right)^2, \tag{3}$$

where $\mathbf{x}_{i,j}^{obs}$ and $\mathbf{x}_{i,j}^{pred}(\xi)$ are the observed and model predicted positions of the i -th multiple image of the j -th background source (N_{fam} is the total number of background sources), respectively.

4. Description of the galaxy cluster strong lensing models

In this section, we briefly describe the lens models for the two galaxy clusters M0416 and A2744. We refer to the papers by Bergamini *et al.* (2023b) and Bergamini *et al.* (2023c) for a detailed description of the models.

4.1. M0416 lens model

The cluster-scale component of M0416 (ϕ^{halo} in Eq. 1) is described as a combination of four non-truncated dual pseudo-isothermal elliptical mass distributions (dPIEs, Limousin *et al.* 2005; Elíasdóttir *et al.* 2007; Bergamini *et al.* 2019). Two elliptical dPIEs have centers close to the position of the two brightest cluster galaxies (BCGs), while a third elliptical dPIE is used to provide second-order corrections to the total mass in the SW region of the cluster. Finally, the fourth circular dPIE is used to account for an over-density of galaxies located NE of the northern BCG. On the whole, the cluster-scale component gives 22 free parameters to the lens model.

For the hot gas component (ϕ^{gas} in Eq. 1), we assume the mass parameterization obtained by Bonamigo *et al.* (2018) from an analysis of the *Chandra* X-ray observations. The latter is described as the sum of four dPIEs and does not add any free parameter to the lens model.

The subhalo mass component of the cluster (ϕ^{gal} in Eq. 1) consists of 212 galaxies parameterized through the scaling relations in Eq. 2. Following the analysis by Bergamini *et al.* (2019), we infer the values of $\alpha = 0.30$ and $\beta_{cut} = 0.60$ from the measured stellar kinematics of 64 member galaxies (down to $mag_{F160W} \sim 22$) that is obtained by fitting the high-quality MUSE galaxy spectra with the software *pPXF* (see Cappellari & Emsellem 2004; Cappellari 2017, 2023). The same measurements are also used to define a Gaussian prior on the normalization σ^{ref} . An additional core-less dPIE is used to describe the cluster galaxy Gal-8971 (as detailed in Bergamini *et al.* 2023b) forming a galaxy-scale strong lensing system. The subhalo mass component adds six more free parameters to the lens model.

Finally, a tSIS profile is used to account for the impact on the lens model coming from a massive foreground galaxy residing in the SW region of the cluster. The galaxy is at a redshift $z = 0.112$. Thus, the cluster lens model is characterized by 30 free parameters that have to be inferred from the observed position of the multiple images.

A careful inspection of the HST photometric and MUSE spectroscopic data allowed us to identify a total of 237 spectroscopically confirmed multiple images from 88 background sources with a redshift range $0.94 \leq z \leq 6.63$. Among the multiple images, we include several multiply imaged substructures of lensed extended sources since these have proven to be extremely useful in constraining the local magnification and the position of the critical lines. We note that this is the largest dataset of secure multiple images ever used in strong gravitational lensing. The observed multiple images provide 298 constraints to the lens model, such that the number of model degree of freedom (dof) is 268.

4.2. A2744 lens model

The cluster-scale component of the A2744 lens model is described by using four dPIEs; two are centered on the two main cluster BCGs, one is located between the two bright galaxies G1 and G2 (see Figure 1), and one is centered on the external galaxy G3. Thus, the cluster-scale component counts a total of 22 free parameters.

The subhalo mass component of the cluster contains a sample of 177 cluster member galaxies, five of which (i.e., the two BCGs and the external galaxies G1, G2, and G3) are modeled as core-less dPIEs (a tSIS is used for G3) and 172 are described through the

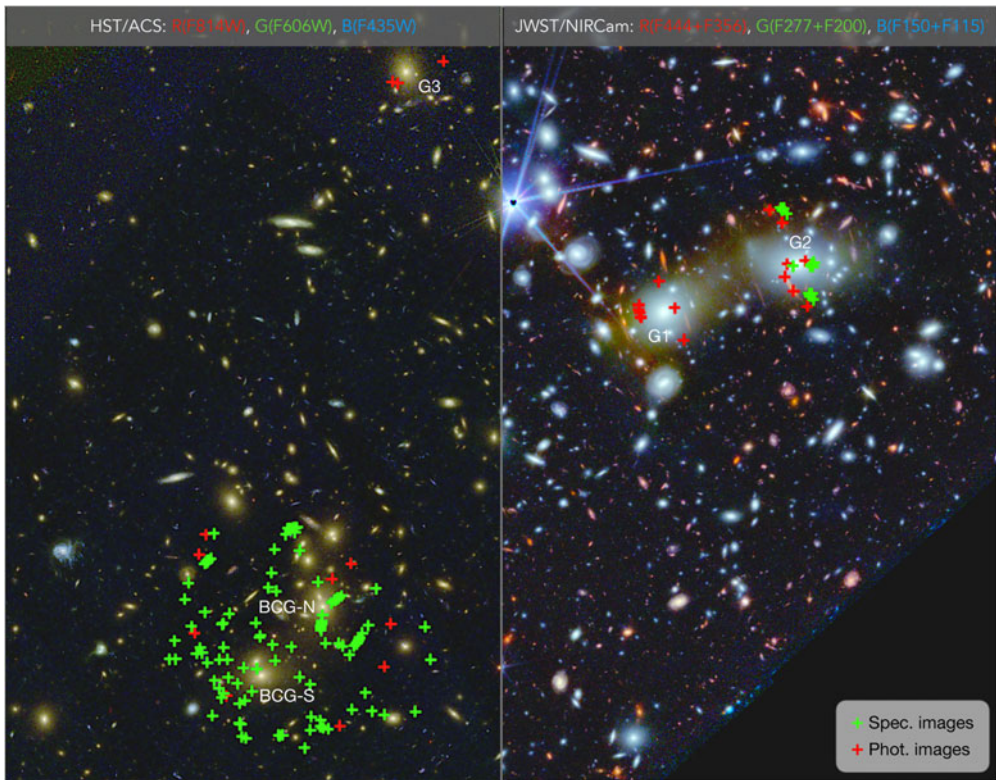


Figure 1. Color-composite merging images of the galaxy cluster A2744. The left half of the image is obtained by a combination of the F814W, F606W, and F435W HST/ACS filters, while the right half of the image is obtained by combining the JWST/NIRCam F444, F356, F277, F200, F150, and F115 filters. The 121 spectroscopically confirmed and the 28 photometric multiple images used in the lens model are marked with green and red crosses, respectively.

scaling relations in Eq. 2. The measured stellar kinematics of 85 member galaxies (down to $mag_{F160W} \sim 22$) is used to determine the slope values $\alpha = 0.40$ and $\beta_{cut} = 0.41$, but none Gaussian prior is assumed on the normalization σ^{ref} .

Thanks to the newly observed JWST/NIRCam images of the cluster and a careful inspection of HST and MUSE data, we were able to identify 149 multiple images from 50 background sources. 121 images are spectroscopically confirmed with a redshift range $1.03 \leq z \leq 9.76$. The redshifts of the remaining 28 photometric images, from 8 background sources, are additional free parameters of the lens model. By considering these 8 additional unknowns, the total number of model free parameter is thus equal to 50, while the multiple images provide 198 constraints to the model (dof=148).

5. Discussion and conclusions

We have presented two high-precision strong lensing models for the galaxy clusters M0416 ($z = 0.396$) and A2744 ($z = 0.307$) based on deep photometric images of the HST and JWST (for A2744) complemented with high-resolution spectroscopic data obtained with MUSE. The lens models are constrained by two of the largest samples of spectroscopically confirmed multiple images ever used in strong gravitational lensing, counting 237 and 149 images for M0416 and A2744, respectively. Both the models have a precision of just $\Delta_{rms} = 0.43''$ in reproducing the position of the multiple images (Bergamini et al. 2023b,c).

In [Bergamini et al. \(2023b\)](#), we presented a comparison between the M0416 lens model described in this work with other published models for the same cluster and exploiting similar data-sets. The comparison is performed by exploiting the *GravityFM* forward modeling code (Bergamini et al. in prep.) to test the capabilities that the different models have in reproducing the observed shapes and magnifications of the surface brightness of several extended lensed galaxies. This analysis demonstrates that our M0416 lens model outperforms all the others in producing accurate deflection and magnification maps even on the scale of the galaxies ([Vanzella et al. 2023](#); [Meštrić et al. 2022](#)). Moreover, the analyses presented in [Bergamini et al. \(2023b\)](#) demonstrate that our model is able to robustly characterize the M0416 total mass distribution.

The large spatial coverage and resolution of the JWST/NIRCam images of A2744 allowed us to identify a large sample of multiple images (149 in total) distributed over an area of ~ 30 arcmin². Remarkably, the photometric redshifts measured for 6 out of 8 of the non-spectroscopic lensed sources included in the model are strongly consistent with the model-predicted redshifts. In the last year, our A2744 lens model was adopted as the reference model by the GLASS-JWST collaboration and was widely used to predict the magnification factors that are necessary to study the physical properties (e.g., star-formation rates, stellar masses, sizes) of the lensed high-*z* galaxies ([Roberts-Borsani et al. 2023](#); [Castellano et al. 2023](#)).

The M0416 and A2744 lens models presented in this work are publicly available at the following link: www.fe.infn.it/astro/lensing/. All model inputs and outputs are accessible through a newly developed Strong Lensing Online Tool (SLOT). This is a user-friendly graphical interface that allows researchers to take full advantage of the statistical results and predictive power of our lens models.

6. Future perspectives

The presented analysis and lens modeling technique will play a fundamental role in the near future when a large number of galaxy cluster lenses are expected to be observed by the JWST and by large area surveys such as the Large Synoptic Survey Telescope (LSST) and *Euclid*. In particular, by combining the magnification power of the cluster lenses with the new generation telescopes (e.g., JWST and ELT) it will be possible to study the physical properties of some of the first sources ensembled in the Universe.

Acknowledgements

Support for program JWST-ERS-1324 was provided by NASA through a grant from the Space Telescope Science Institute, which is operated by the Association of Universities for Research in Astronomy, Inc., under NASA contract NAS 5-03127. The Hubble Frontier Field program (HFF) and the Beyond Ultra-deep Frontier Fields And Legacy Observations (BUFFALO) are based on the data made with the NASA/ESA *Hubble Space Telescope*. The Space Telescope Science Institute is operated by the Association of Universities for Research in Astronomy, Inc., under NASA contract NAS 5-26555. ACS was developed under NASA Contract NAS 5-32864. Based also on observations collected at the European Southern Observatory for Astronomical research in the Southern Hemisphere under ESO programmes with IDs 094.A-0115 (PI: Richard). We acknowledge financial support through grants PRIN-MIUR 2015W7KAWC, 2017WSCC32, and 2020SKSTHZ. AA has received funding from the European Union's Horizon 2020 research and innovation programme under the Marie Skłodowska-Curie grant agreement No 101024195 - ROSEAU. GBC thanks the Max Planck Society for support through the Max Planck Research Group for S. H. Suyu and the academic support from the German Centre

for Cosmological Lensing. MM acknowledges support from the Italian Space Agency (ASI) through contract “Euclid - Phase D”.

References

- Angora, G., Rosati, P., Brescia, M., et al. 2020, *A&A*, 643, A177. doi:10.1051/0004-6361/202039083
- Bacon, R., Accardo, M., Adjali, L., et al. 2012, *The Messenger*, 147, 4
- Bergamini, P., Acebron, A., Grillo, C., et al. 2023, *ApJ*, 952, 84. doi:10.3847/1538-4357/acd643
- Bergamini, P., Grillo, C., Rosati, P., et al. 2023, *A&A*, 674, A79. doi:10.1051/0004-6361/202244834
- Bergamini, P., Rosati, P., Mercurio, A., et al. 2019, *A&A*, 631, A130. doi:10.1051/0004-6361/201935974
- Bergamini, P., Rosati, P., Vanzella, E., et al. 2021, *A&A*, 645, A140. doi:10.1051/0004-6361/202039564
- Bergamini, P., Acebron, A., Grillo, C., et al. 2023, *A&A*, 670, A60. doi:10.1051/0004-6361/202244575
- Bezanson, R., Labbe, I., Whitaker, K. E., et al. 2022, arXiv:2212.04026. doi:10.48550/arXiv.2212.04026
- Bonamigo, M., Grillo, C., Ettori, S., et al. 2018, *ApJ*, 864, 98. doi:10.3847/1538-4357/aad4a7
- Caminha, G. B., Grillo, C., Rosati, P., et al. 2016, *A&A*, 587, A80. doi:10.1051/0004-6361/201527670
- Caminha, G. B., Rosati, P., Grillo, C., et al. 2019, *A&A*, 632, A36. doi:10.1051/0004-6361/201935454
- Cappellari, M. & Emsellem, E. 2004, *PASP*, 116, 138. doi:10.1086/381875
- Cappellari, M. 2017, *MNRAS*, 466, 798. doi:10.1093/mnras/stw3020
- Cappellari, M. 2023, *MNRAS*. doi:10.1093/mnras/stad2597
- Castellano, M., Fontana, A., Treu, T., et al. 2023, *ApJ*, 948, L14. doi:10.3847/2041-8213/accea5
- Eliasdóttir, Á., Limousin, M., Richard, J., et al. 2007, arXiv:0710.5636. doi:10.48550/arXiv.0710.5636
- Grillo, C., Karman, W., Suyu, S. H., et al. 2016, *ApJ*, 822, 78. doi:10.3847/0004-637X/822/2/78
- Jullo, E., Kneib, J.-P., Limousin, M., et al. 2007, *New Journal of Physics*, 9, 447. doi:10.1088/1367-2630/9/12/447
- Jullo, E. & Kneib, J.-P. 2009, *MNRAS*, 395, 1319. doi:10.1111/j.1365-2966.2009.14654.x
- Karman, W., Caputi, K. I., Caminha, G. B., et al. 2017, *A&A*, 599, A28. doi:10.1051/0004-6361/201629055
- Kneib, J.-P., Ellis, R. S., Smail, I., et al. 1996, *ApJ*, 471, 643. doi:10.1086/177995
- Lagattuta, D. J., Richard, J., Clément, B., et al. 2017, *MNRAS*, 469, 3946. doi:10.1093/mnras/stx1079
- Le Fèvre, O., Saisse, M., Mancini, D., et al. 2003, *Proc. SPIE*, 4841, 1670. doi:10.1117/12.460959
- Limousin, M., Kneib, J.-P., & Natarajan, P. 2005, *MNRAS*, 356, 309. doi:10.1111/j.1365-2966.2004.08449.x
- Lotz, J. M., Koekemoer, A., Coe, D., et al. 2017, *ApJ*, 837, 97. doi:10.3847/1538-4357/837/1/97
- Mahler, G., Richard, J., Clément, B., et al. 2018, *MNRAS*, 473, 663. doi:10.1093/mnras/stx1971
- Meštrić, U., Vanzella, E., Zanella, A., et al. 2022, *MNRAS*, 516, 3532. doi:10.1093/mnras/stac2309
- Postman, M., Coe, D., Benítez, N., et al. 2012, *ApJS*, 199, 25. doi:10.1088/0067-0049/199/2/25
- Richard, J., Claeysens, A., Lagattuta, D., et al. 2021, *A&A*, 646, A83. doi:10.1051/0004-6361/202039462
- Roberts-Borsani, G., Treu, T., Chen, W., et al. 2023, *Nature*, 618, 480. doi:10.1038/s41586-023-05994-w
- Steinhardt, C. L., Jauzac, M., Acebron, A., et al. 2020, *ApJS*, 247, 64. doi:10.3847/1538-4365/ab75ed
- Treu, T., Roberts-Borsani, G., Bradac, M., et al. 2022, *ApJ*, 935, 110. doi:10.3847/1538-4357/ac8158

- Vanzella, E., Castellano, M., Bergamini, P., et al. 2022, ApJ, 940, L53. doi:10.3847/2041-8213/ac8c2d
- Vanzella, E., Castellano, M., Meneghetti, M., et al. 2017, ApJ, 842, 47. doi:10.3847/1538-4357/aa74ae
- Vanzella, E., Meneghetti, M., Caminha, G. B., et al. 2020, MNRAS, 494, L81. doi:10.1093/mnrasl/slaa041
- Vanzella, E., Caminha, G. B., Rosati, P., et al. 2021, A&A, 646, A57. doi:10.1051/0004-6361/202039466
- Vanzella, E., Loiacono, F., Bergamini, P., et al. 2023, arXiv:2305.14413. doi:10.48550/arXiv.2305.14413